ACS OMEGA

Open Access

http://pubs.acs.org/journal/acsodf

Article

Structural Transitions in Complementary G-Rich and C-Rich Strands and Their Mixture at Various pH Conditions

Milena Kh. Badalyan, Ishkhan V. Vardanyan,* Samvel G. Haroutiunian, and Yeva B. Dalyan

Cite This: *ACS Omega* 2023, 8, 47051−47056

Read Online

ACCESS | Metrics & More | Article Recommendations

ABSTRACT: We used circular dichroism spectroscopy, UV spectrophotometry, and differential scanning calorimetry to investigate pH-dependent structural transitions in an equimolar mixture of complementary G-rich d[5′-A(GGGTTA)$_3$GGG-3′] (TelG) and C-rich d[3′-T(CCCAAT)$_3$CCC-5′] (TelC) human telomeric DNA strands. Our studies were conducted at neutral (pH 7.0) and slightly acidic (pH 5.5 and 6.5) pH. We analyzed the melting thermodynamics of TelG and TelC and their equimolar mixture. Our analysis revealed that the preferred conformation of an equimolar mixture of TelG and TelC is the duplex. At pH 5.5, however, in addition to the duplex state, we observed a significant population of the *i*-motif state formed by TelC. Our results are consistent with the picture in which an increase in pH from 5.5 to 7.0 has little effect on the melting enthalpy of an isolated G-quadruplex while causing a strong reduction in the melting enthalpy of an isolated *i*-motif (the latter diminishes to 0 at pH 7.0). These effects summarily lead to a decrease in the contribution of the *i*-motif to the melting enthalpy of the mixture and, hence, an increase in the apparent melting enthalpy and overall stability of the duplex state.

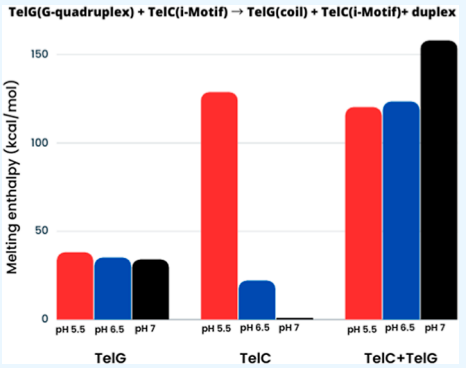

INTRODUCTION

It is known that genomic DNA predominantly exists as Watson−Crick double helix (B-DNA). However, during cellular processes, DNA strands within specific regions of genomic DNA (such as telomeres, promoter regions of oncogenes, etc.) can form four-stranded G-quadruplex or *i*-motif structures.[1−14] G-quadruplexes are formed by G-rich DNA strands. They involve planar structures called G-quartets, which consist of four guanines interconnected via Hoogsteen hydrogen bonds.[1−8] In a weakly acidic solution, C-rich DNA sequences, which by definition are complementary to G-rich strands, can fold into an *i*-motif, an alternative four-stranded DNA structure stabilized by a hemiprotonated C−C$^+$ base pair.[9−13] The three-dimensional structures of G-quadruplexes and *i*-motifs differ significantly from that of a duplex (the former are globular shaped with a smaller charge density). Formation of four-stranded noncanonical structures in the genome creates steric hindrances to the function of RNA polymerase and telomerase, which, in turn, may interfere with gene expression and even lead to cell death.[15−23] The discovery of this fact became the basis for the development of novel strategies of anticancer therapy, which are based on the targeted induction or destruction of G-quadruplexes and *i*-motifs at preselected genomic sites.[18−20,22]

To elucidate the biological role of molecular switches in the genome, an understanding of the balance of the forces that stabilize or destabilize canonical and noncanonical DNA conformations becomes of central importance. The formation of four-stranded G-quadruplex or *i*-motif structures within a genomic site in vivo requires unfolding of the double helix with the subsequent folding of dissociating strands into four-stranded conformations (i.e., double helix → single-stranded coils → four-stranded conformations). The resulting distribution of conformation states should depend on the nucleotide sequence and on environmental conditions (temperature, pH, cosolvents, ligands, etc.).[23−29] pH is of particular importance for the formation of an *i*-motif by the C-rich DNA strand as its stability is strongly pH-dependent with the maximum observed at slightly acidic pH. In general, the conformational preferences of the system of complementary G-rich and C-rich DNA strands are governed by the relative free energies, ΔG°, of the single-, double-, and four-stranded conformations.[23−28]

MATERIALS

The 22-base d[3′-T(CCCAAT)$_3$CCC-5′] (TelC) and d[5′-A(GGGTTA)$_3$GGG-3′] (TelG) human telomeric DNA strands were purchased from Integrated DNA Technologies (Coralville, Iowa, USA) and used without further purification.

Received: September 11, 2023
Revised: October 11, 2023
Accepted: November 14, 2023
Published: November 28, 2023

The experiments at pH 5.5 were carried out in a Na−acetate buffer, while those at pH 6.5 and 7.0 were conducted in a Na−phosphate buffer.

The concentrations of TelC and TelG were determined spectrophotometrically by measuring UV light absorbance at 260 nm at 80 °C and using extinction coefficients, ε_{260}, of 228,500 and 194,600 M^{-1} cm^{-1} for TelG and TelC, respectively. A Lambda-800 (PerkinElmer) UV/vis spectrophotometer was used for all spectrophotometric measurements.

The conformational changes of TelC and TelG were studied by measuring their circular dichroism (CD) spectra with a DSM 20 (Olis, USA) CD spectrophotometer.

The calorimetric investigations were carried out with a Nano-DSC (TA Instruments) microcalorimeter with a cell volume of 300 μL. Calorimetric heating was carried out according to the following protocol; the sample was cooled to 5 °C, equilibrated for 10 min, and then heated to 90 °C at a rate of 1 °C per minute. Changes in enthalpy, entropy, and Gibbs free energy were calculated from the DSC melting profiles (thermograms) using the following standard formulas

$$\Delta H^0(T_m) = \int_{T_i}^{T_f} C_p^0 \, dT$$

$$\Delta S^0(T_m) = \int_{T_i}^{T_f} \frac{C_p^0}{T} dT$$

$$\Delta G^0(T) = \Delta H^0(T) - T\Delta S^0(T) \quad (1)$$

RESULTS AND DISCUSSION

In this work, we investigated the structural transitions within an equimolar mixture of complementary G-rich d[5′-A-$(GGGTTA)_3$GGG-3′] (TelG) and C-rich d[5′CCC-$(TAACCC)_3$T-3′] (TelC) human telomeric DNA at pH ranging from slightly acidic to neutral (pH 5.5, 6.5, and 7.0). The slightly acidic solution is a prerequisite for *i*-motif formation by TelC (Figure 1). We analyzed our data to determine the temperature dependencies of the thermodynamic parameters of the stability of the canonical and noncanonical conformations adopted by the TelG and TelC DNA strands.

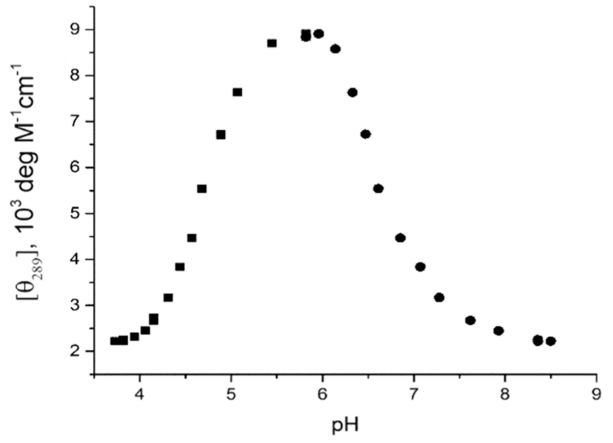

Figure 1. pH dependence of the molar ellipticity of TelC at 289 nm. The CD band centered at 289 nm is characteristic of the *i*-motif formation by TelC.

Spectral Investigations. Information about the pH-dependent conformational rearrangements of TelC and TelG and their equimolar mixtures (TelC + TelG) can be obtained from CD spectral measurements. Figure 2 shows the CD spectra of TelC and TelG, and their equimolar mixture at pH 5.5 (panel A), 6.5 (panel B), and 7.0 (panel C).

As can be seen from Figure 2a, at pH 5.5, TelC folds into a stable *i*-motif structure with a positive CD band with a maximum at 290 nm and a negative band with a minimum at 257 nm (shown in red).[24] An increase in pH destabilizes the *i*-motif formed by TelC because of a decrease in the level of cytosine protonation. At pH 6.5 (Figure 2b), the intensity of the *i*-motif bands decreases, and the positions of the characteristic CD bands change (the positive band shifts to 280 nm, while the negative band shifts to 250 nm). This observation may suggest that at pH 6.5, TelC exists in a mixed *i*-motif-plus-coil conformational state. At pH 7.0 (Figure 2c), the band intensities are greatly reduced with a further blue shift in their positions (the positive and negative bands are centered at 275 and 245 nm, respectively). This observation suggests that, at pH 7.0, TelC does not form any *i*-motif but exists in the single-stranded coiled state.

The CD spectra of TelG shown in Figure 2a−c (marked in black) reveal that, at all experimental values of pH, TelG adopts the G-quadruplex conformation (with a maximum at 295 nm and a minimum at 265 nm).[24,25]

At pH 5.5, the CD spectrum of an equimolar solution of TelG and TelC (marked in green in Figure 2a) showed significant kinetics taking 5 h to reach equilibrium after mixing. Relatively slow folding kinetics was observed also at pH 6.5 and 7.0 with equilibration times of 1.5 and 0.5 h, respectively. At all experimental pHs, the equilibrium CD spectra of the mixture (Figure 2a−c) did not alter remaining the same for the next 24 h. The longer folding kinetics observed at pH 5.5 can be explained by TelC being initially in the *i*-motif state and the large activation energy between the *i*-motif and duplex states. At pH 6.5 and 7.0, the folding kinetics is determined by the activation energy between the G-quadruplex (the premixing state of TelG) and duplex states.

Inspection of Figure 2 reveals that, at all experimental pHs, the equilibrium CD spectrum of an equimolar mixture of TelG and TelC has a maximum at about 267 nm and a minimum at about 240 nm, a characteristic spectral feature of double-stranded DNA.[24] The prevalence of the duplex structure is also suggested by UV melting profiles (heating and subsequent cooling) of an equimolar mixture of TelG and TelC carried out 24 h after the mixing. Figure 3 shows the melting and annealing curves for an equimolar mixture of TelG and TelC measured at 295 nm in a pH 5.5 solution.

The complex melting and annealing behavior in Figure 3 can be rationalized as follows. The low-temperature hypochromic transition with a midpoint of ∼40 °C corresponds to the melting of the *i*-motif formed by TelC; the hyperchromic transitions with a midpoint of 70 °C corresponds to the melting of the TelG/TelC duplex; and the high-temperature hypochromic transition with a midpoint of ∼75 °C corresponds to the melting of the G-quadruplex formed by TelG.[25,26] Thus, judging by the melting profile presented in Figure 3, we conclude that the duplex, G-quadruplex, and *i*-motif conformations coexist in equimolar mixtures of TelG and TelC at pH 5.5.

In the next section, we use differential scanning calorimetric (DSC) measurements to further characterize the thermody-

https://doi.org/10.1021/acsomega.3c06934
ACS Omega 2023, 8, 47051−47056

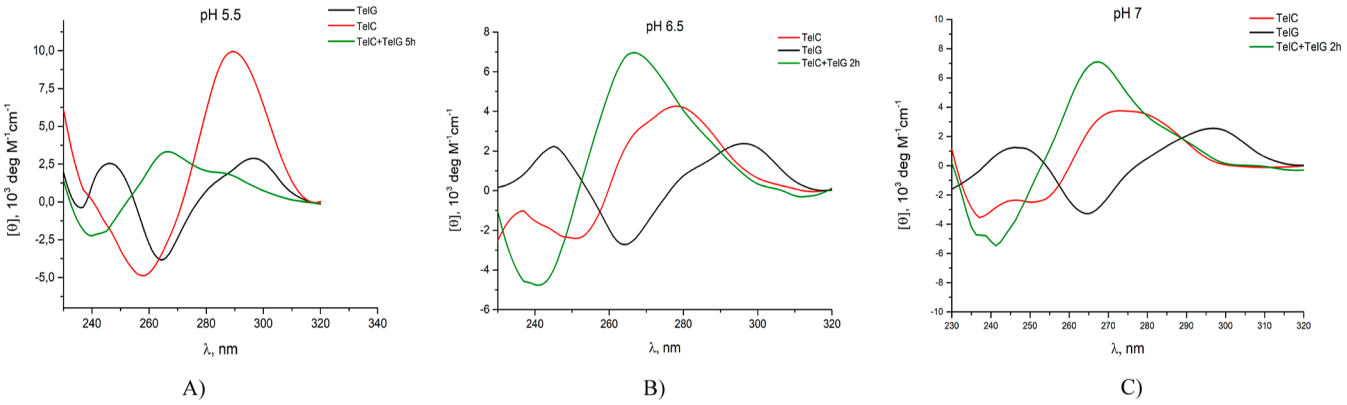

Figure 2. CD spectra of TelG (black), TelC (red), and an equimolar mixture of TelG and TelC (green) at pH 5.5 and 5 h after the mixing (panel A); pH 6.5 and 1.5 h after the mixing (panel B); and pH 7.0 and 0.5 h after the mixing (panel C).

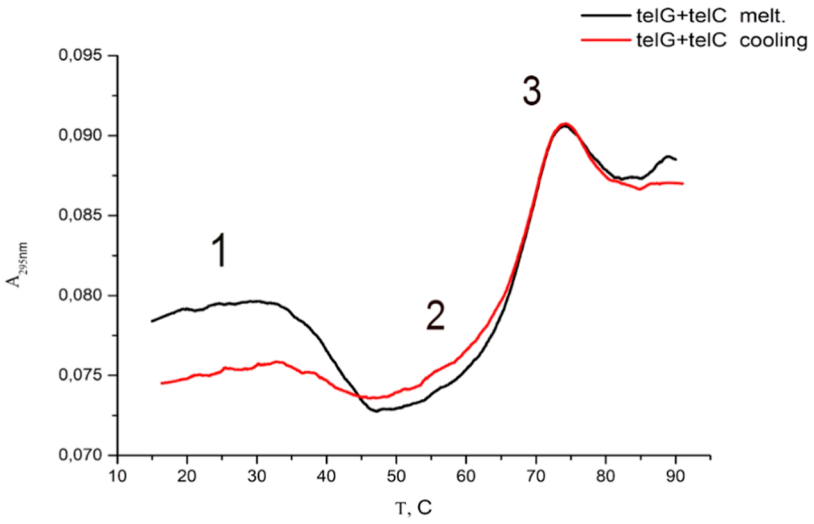

Figure 3. 295 nm UV heating (black) and cooling (red) profiles of an equimolar mixture of TelG and TelC at pH 5.5.

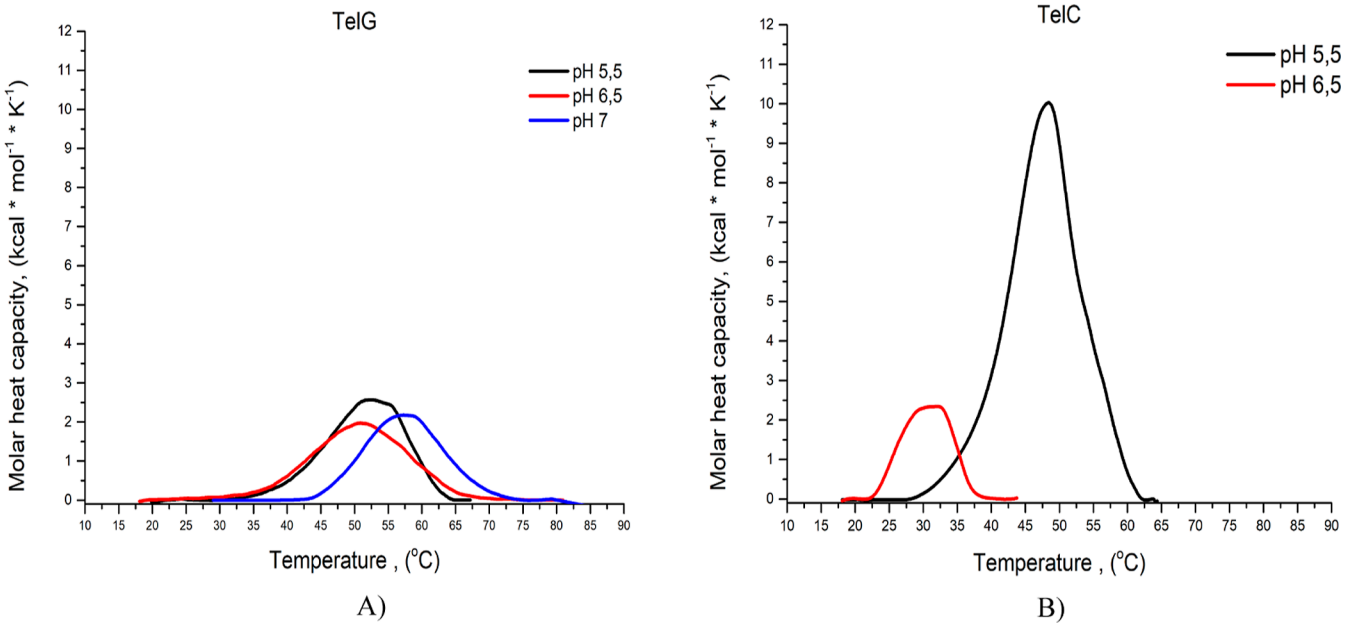

Figure 4. DSC thermograms of TelG at pH 5.5 (black), pH 6.5 (red), and pH 7.0 (blue) (A) and TelC at pH 5.5 (black) and pH 6.5 (red) (B).

namics of conformational interconversions of TelG, TelC, and their equimolar mixture.[30−33]

Differential Scanning Calorimetry. Figure 4 presents the DSC thermograms for TelG at pH 5.5, 6.5, and 7.0 (panel A)

https://doi.org/10.1021/acsomega.3c06934
ACS Omega 2023, 8, 47051−47056

Table 1. Thermodynamic Parameters of the Melting Transitions of TelG and TelC at Different pH

pH	ΔG (kcal/mol)		ΔH (kcal/mol)		Δs (kcal/mol K)		T_{max} (°C)	
	TelG	TelC	TelG	TelC	TelG	TelC	TelG	TelC
pH 5.5	2.2 ± 0.01	3.1 ± 0.2	38.0 ± 0.3	128.5 ± 1.1	0.11 ± 0.01	0.39 ± 0.02	52.3 ± 0.1	48.5 ± 0.1
pH 6.5	0.01 ± 0.002	0.8 ± 0.03	35.0 ± 0.3	22.1 ± 0.2	0.11 ± 0.01	0.07 ± 0.003	51.8 ± 0.1	32.0 ± 0.1
pH 7.0	0.35 ± 0.01		33.4 ± 0.3		0.10 ± 0.01		57.5 ± 0.1	

and TelC at pH 5.5 and 6.5 (panel B). All DSC measurements were carried out at 100 mM NaCl. Recall that, under these solution conditions and low temperatures, TelG adopts the G-quadruplex conformation, while TelC adopts the *i*-motif conformation. Table 1 shows the thermodynamic parameters of the melting transitions of TelG and TelC derived from our DSC measurements.

Inspection of calorimetric data on TelG presented in Figure 4a and Table 1 reveals that an increase in pH from 5.5 to 7.0 leads to an increase in T_m from 52.3 ± 0.1 °C to 57.5 ± 0.1 °C and a decrease in melting enthalpy (ΔH) from 38 ± 0.3 to 33.4 ± 0.3 kcal/mol. In other words, an increase in pH to neutral values makes the G-quadruplex formed by TelG more thermostable, albeit with a lower differential free energy of the folded and unfolded conformations.

In contrast to the G-quadruplex, an increase in pH strongly destabilizes the *i*-motif formed by TelC (see Figure 4b). At pH 5.5, there is a strong calorimetric peak at 48.5 ± 0.1 °C with a melting enthalpy, ΔH, of 128.5 ± 1.1 kcal/mol. At pH 6.5, the diminished peak shifts to a lower temperature of 32 ± 0.1 °C with a ΔH of 22.1 ± 0.2 kcal/mol (Table 1). Judging by the ratio of melting enthalpies, only ∼17% (=22.1/128) of the TelC population forms an *i*-motif at pH 6.5. At pH 7.0, TelC does not manifest any calorimetric melting, consistent with its being in the coil state.

Figure 5 presents DSC thermograms for an equimolar mixture of TelC and TelG (blue) at pH 5.5 (A), 6.5 (B), and 7.0 (panel C). For comparison, Figure 5a−c also shows the heat capacity melting profiles of TelG (black) and TelC (red) at respective pH. We carried out the DSC measurements in equimolar mixtures of TelG and TelC 24 h after mixing. Table 2 shows the thermodynamic parameters of the melting transitions of an equimolar mixture of TelG and TelC.

Our combined UV melting and CD results suggest that, although the duplex is the main conformation of an equimolar mixture of TelG and TelC, the G-quadruplex, *i*-motif, and coil conformations also may be present at ratios depending on the solution pH. As explained below, DSC results can be used to estimate the fractional populations and energetics of conformational states present in the mixture.

At pH 5.5, the thermogram of the mixture of TelG and TelC exhibits two calorimetric peaks with melting temperatures of 49.1 ± 0.1 and 62.7 ± 0.1 °C (Figure 5a). This observation is consistent with the presence of two equilibrium structures with melting profiles well separated along the temperature axis. The smaller peak centering at 49.1 ± 0.1 °C (see Table 2) corresponds to the melting temperatures of isolated G-quadruplex (T_m = 52.3 ± 0.1 °C) and of *i*-motif (T_m = 48.5 ± 0.1 °C) structures (see Table 1). Recall that the *i*-motif manifests its maximum stability at pH 5.5. Relative to the *i*-motif, the enthalpic contribution of the G-quadruplex formed by TelG is more modest since its melting enthalpy is ∼3.5 times smaller than that of the *i*-motif formed by TelC (Table 1). Interestingly, the melting enthalpy of an isolated *i*-motif of 128.5 ± 1.1 kcal/mol is higher than the melting enthalpy of the

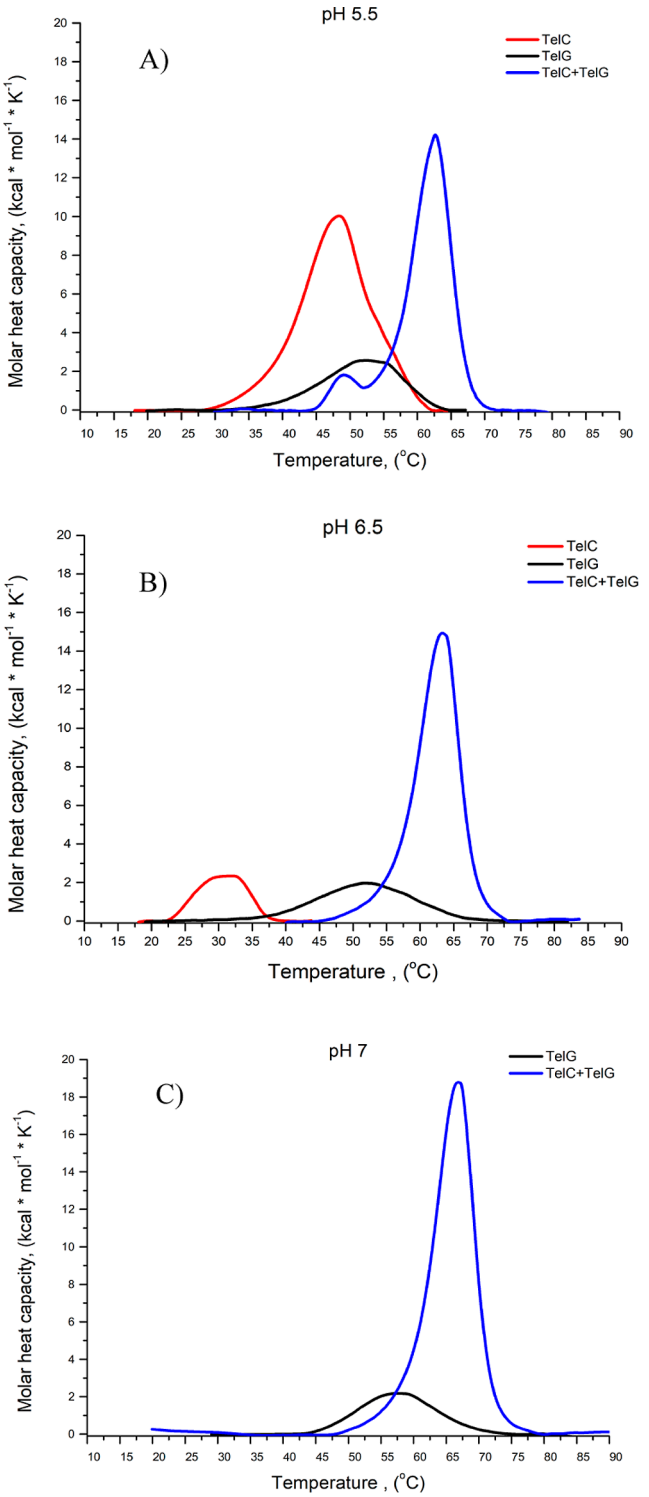

Figure 5. DSC thermograms for TelG (black), TelC (red), and an equimolar mixture of TelC and TelG (blue) at pH 5.5 (A), 6.5 (B), and pH 7.0 (panel C).

https://doi.org/10.1021/acsomega.3c06934
ACS Omega 2023, 8, 47051−47056

Table 2. Thermodynamic Parameters of the Melting Transitions of an Equimolar Mixture of TelG and TelC

pH	ΔG (kcal/mol)	ΔH (kcal/mol)	$T\Delta S$ (kcal/mol)	T_{max} (°C)
pH 5.5	0.2 ± 0.03	110.9 ± 1.9 (total)	110.9 ± 1.9	49.1 ± 0.1 (1st peak)
		9.1 ± 0.5 (1st peak)		62.7 ± 0.1 (2nd peak)
pH 6.5	2.0 ± 0.11	123.1 ± 1.2	121.1 ± 1.5	63.4 ± 0.1
pH 7.0	1.3 ± 0.1	157.7 ± 1.5	114.1 ± 1.7	66.8 ± 0.1

mixture of TelG and TelC of 110.9 ± 1.9 kcal/mol although the latter melts at a higher temperature (Table 2). We propose that the low-temperature calorimetric peak in Figure 4a reflects the melting of a small population of the G-quadruplex and *i*-motif structures formed by TelG and TelC, respectively. The high-temperature (main) peak with a T_m of 62.7 ± 0.1 °C reflects the melting of the duplex formed by the complementary TelG and TelC strands.

At pH 6.5, the thermogram for the TelG-plus-TelC mixture manifests a single peak (Figure 5b). We propose that this peak corresponds to the melting of the duplex formed by the associating TelG and TelC strands. Inspection of the DSC data presented in Table 2 reveals that the melting temperature and enthalpy of duplex melting at pH 6.5 are only very slightly higher than those observed at pH 5.5. This observation is consistent with the relative pH-independence of the thermodynamics of duplex-to-single strand transitions in neutral to mildly acidic solutions. Relative to pH 6.5, the single-peak melting profile of the TelG-plus-TelC mixture at pH 7.0 shown in Figure 5c shifts to a higher temperature of 66.8 ± 0.1 °C and exhibits a higher enthalpy of 157.7 ± 1.5 kcal/mol (see Table 2). Similarly to the situation at pH 6.5, we propose that the DSC thermogram at pH 7.0 is representative of duplex melting with no contribution from the melting of the four-stranded structures.

Our results are consistent with the picture in which an increase in pH from 5.5 to 7.0 has little effect on the melting enthalpy of an isolated G-quadruplex while causing a strong reduction in the melting enthalpy of an isolated *i*-motif (the latter diminishes to 0 at pH 7.0). These effects summarily lead to a decrease in the contribution of the *i*-motif to the melting enthalpy of the mixture and, hence, an increase in the apparent melting enthalpy and overall stability of the duplex state.

In summary, we characterized the pH-dependent kinetics and thermodynamics of the formation of a duplex structure by human telomeric TelG and TelC strands. We interpret our results within the framework of an interplay between the duplex, G-quadruplex, *i*-motif, and coil conformations adopted by the complementary TelG and TelC strands.

AUTHOR INFORMATION

Corresponding Author

Ishkhan V. Vardanyan − *Department of Molecular Physics, Yerevan State University, Yerevan 0025, Armenia;* orcid.org/0000-0002-7568-0237; Email: ishkhan@ysu.am

Authors

Milena Kh. Badalyan − *Department of Molecular Physics, Yerevan State University, Yerevan 0025, Armenia*

Samvel G. Haroutiunian − *Department of Molecular Physics, Yerevan State University, Yerevan 0025, Armenia*

Yeva B. Dalyan − *Department of Molecular Physics, Yerevan State University, Yerevan 0025, Armenia*

Complete contact information is available at: https://pubs.acs.org/10.1021/acsomega.3c06934

Notes

The authors declare no competing financial interest.

ACKNOWLEDGMENTS

This work was supported by the Science Committee of the Ministry of Education, Science, Culture, and Sport of the Republic of Armenia under grant no. 21T-1F115.

REFERENCES

(1) Huppert, J. L. Four-stranded nucleic acids: structure, function and targeting of G-quadruplexes. *Chem. Soc. Rev.* **2008**, *37*, 1375−1384.

(2) Li, W.; Wu, P.; Ohmichi, T.; Sugimoto, N. Characterization and thermodynamic properties of quadrupex/duplex competition. *FEBS Lett.* **2002**, *526*, 77−81.

(3) Hansel-Hertsch, R.; Di Antonio, M.; Balasubramanian, S. DNA G-quadruplexes in the human genome: detection, functions and therapeutic potential. *Nat. Rev. Mol. Cell Biol.* **2017**, *18*, 279−284.

(4) Tateishi-Karimata, H.; Sugimoto, N. Chemical biology of non-canonical structures of nucleic acids for therapeutic applications. *Chem. Commun.* **2020**, *56*, 2379−2390.

(5) Sugimoto, N. Noncanonical structures and their thermodynamics of DNA and RNA under molecular crowding: beyond the Watson-Crick double helix. *Int. Rev. Cell. Mol. Biol.* **2014**, *307*, 205−273.

(6) Huppert, J. L. Structure, location and interactions of G-quadruplexes. *FEBS J.* **2010**, *277*, 3452−3458.

(7) Qin, Y.; Hurley, L. H. Structures, folding patterns, and functions of intramolecular DNA G-quadruplexes found in eukaryotic promoter regions. *Biochimie* **2008**, *90*, 1149−1171.

(8) Day, H. A.; Pavlou, P.; Waller, Z. A. i-Motif DNA: structure, stability and targeting with ligands. *Bioorg. Med. Chem.* **2014**, *22*, 4407−4418.

(9) Benabou, S.; Avino, A.; Eritja, R.; Gonzalez, C.; Gargallo, R. Fundamental aspects of the nucleic acid i-motif structures. *RSC Adv.* **2014**, *4*, 26956−26980.

(10) Alba, J. J.; Sadurni, A.; Gargallo, R. Nucleic acid i-motif structures in analytical chemistry. *Crit. Rev. Anal. Chem.* **2016**, *46*, 443−454.

(11) Gehring, K.; Leroy, J. L.; Gueron, M. A. A tetrameric DNA structure with protonated cytosine-cytosine base pairs. *Nature* **1993**, *363*, 561−565.

(12) Mergny, J. L.; Lacroix, L.; Han, X. G.; Leroy, J. L.; Helene, C. Intramolecular folding of pyrimidine oligodeoxynucleotides into an i-DNA motif. *J. Am. Chem. Soc.* **1995**, *117*, 8887−8898.

(13) Kim, B. G.; Chalikian, T. V. Thermodynamic linkage analysis of pH-induced folding and unfolding transitions of i-motifs. *Biophys. Chem.* **2016**, *216*, 19−22.

(14) Sanchez-Martin, V. DNA G-Quadruplex-Binding Proteins: An Updated Overview. *DNA* **2023**, *3*, 1−12.

(15) De Cian, A.; Lacroix, L.; Douarre, C.; Temime-Smaali, N.; Trentesaux, C.; Riou, J. F.; Mergny, J. L. Targeting telomeres and telomerase. *Biochimie* **2008**, *90*, 131−155.

(16) Hurley, L. H. DNA and its associated processes as targets for cancer therapy. *Nat. Rev. Cancer* **2002**, *2*, 188−200.

(17) Sun, D.; Hurley, L. H. The importance of negative superhelicity in inducing the formation of G-quadruplex and i-motif structures in

the c-MYC promoter: implications for drug targeting and control of gene expression. *J. Med. Chem.* **2009**, *52*, 2863−2874.
(18) Oganesian, L.; Bryan, T. M. Physiological relevance of telomeric G-quadruplex formation: a potential drug target. *BioEssays* **2007**, *29*, 155−165.
(19) Balasubramanian, S.; Hurley, L. H.; Neidle, S. Targeting G-quadruplexes in gene promoters: a novel anticancer strategy? *Nat. Rev. Drug Discovery* **2011**, *10*, 261−275.
(20) Maizels, N. G4-associated human diseases. *EMBO Rep.* **2015**, *16*, 910−922.
(21) Brooks, T. A.; Kendrick, S.; Hurley, L. Making sense of G-quadruplex and i-motif functions in oncogene promoters. *FEBS J.* **2010**, *277*, 3459−3469.
(22) Collie, G. W.; Parkinson, G. N. The application of DNA and RNA G-quadruplexes to therapeutic medicines. *Chem. Soc. Rev.* **2011**, *40*, 5867−5892.
(23) Xu, Y.; Sugiyama, H. Formation of the G-quadruplex and i-motif structures in retinoblastoma susceptibility genes (Rb). *Nucleic Acids Res.* **2006**, *34*, 949−954.
(24) Liu, L.; Ma, C.; Wells, J. W.; Chalikian, T. V. Conformational preferences of DNA strands from the promoter region of the c-MYC oncogene. *J. Phys. Chem. B* **2020**, *124*, 751−762.
(25) Aslanyan, L.; Ko, J.; Kim, B. G.; Vardanyan, I.; Dalyan, Y. B.; Chalikian, T. V. Effect of urea on G-quadruplex stability. *J. Phys. Chem. B* **2017**, *121*, 6511−6519.
(26) Dalyan, Ye. B.; Aslanyan, L. G.; Vardanyan, I. V. The influence of urea on G-quadruplex and I-motif structures in complementary DNA sequences. *Proceedings of YSU, Physical and Mathematical Sciences* **2020**, *54*, 115−122.
(27) Chalikian, T. V.; Liu, L.; Macgregor, R. B., Jr. Duplex-tetraplex equilibria in guanine- and cytosine-rich DNA. *Biophys. Chem.* **2020**, *267*, 106473.
(28) Phan, A. T.; Mergny, J.-L. Human telomeric DNA: G-quadruplex, i-motif and Watson-Crick double helix. *Nucleic Acids Res.* **2002**, *30* (21), 4618−4625.
(29) Abou Assi, H.; El-Khoury, R.; Gonzalez, C.; Damha, M. J. 2-Fluoroarabinonucleic acid modification traps G-quadruplex and i-motif structures in human telomeric DNA. *Nucleic Acids Res.* **2017**, *45* (20), 11535−11546.
(30) Kaushik, M.; Suehl, N.; Marky, L. A. Calorimetric unfolding of the bimolecular and i-motif complexes of the human telomere complementary strand, $d(C_3TA_2)_4$. *Biophys. Chem.* **2007**, *126*, 154−164.
(31) Klump, H.; Burkart, W. Calorimetric measurements of the transition enthalpy of DNA in aqueous urea solutions. *Biochim. Biophys. Acta* **1977**, *475*, 601−604.
(32) Hadzi, S.; Boncina, M.; Lah, J. G-Quadruplex Stability from DSC Measurements. In *G-Quadruplex Nucleic Acids: Methods and Protocols, Methods in Molecular Biology*; Yang, D., Lin, C., Eds.; Springer, 2019; Vol. *2035*, pp 117−130.
(33) Pagano, B.; Randazzo, A.; Fotticchia, I.; Novellino, E.; Petraccone, L.; Giancola, C. Differential scanning calorimetry to investigate G-quadruplexes structural stability. *Methods* **2013**, *64* (1), 43−51.

https://doi.org/10.1021/acsomega.3c06934
ACS Omega 2023, 8, 47051−47056